Chapter 8: Treatment of trophoblastic disease

CQ43 What chemotherapy is recommended for an invasive mole, clinical invasive mole, or post-molar persistent human chorionic gonadotropin (hCG)?

Recommendations:

Monotherapy with methotrexate or actinomycin D is recommended (Grade B).

CQ44 What chemotherapy is recommended for choriocarcinoma?

Recommendations:

A multidrug regimen including methotrexate, actinomycin D, and etoposide is recommended (Grade C1).

[See Fig. 9].

CQ45 What are the indications for surgery for choriocarcinoma?

Recommendations:

1. Surgical resection is considered for patients with a uterine lesion or metastatic lesion associated with chemoresistance (Grade C1).
2. Surgical resection is also considered for patients with a uterine lesion in which hemorrhage is difficult to control or those who have brain metastasis with symptoms of intracranial hypertension (Grade C1).

[See Fig. 9].

CQ46 What are the indications for radiation therapy for choriocarcinoma?

Recommendations:

Whole-brain irradiation and/or stereotactic radiosurgery are considered to treat brain metastasis (Grade C1).

[See Fig. 9].

CQ47 What treatments are recommended for cases with placental site trophoblastic disease or epithelioid trophoblastic tumor?

Recommendations:

1. Total hysterectomy is recommended for patients with disease limited to the uterus (Grade B).
2. Combination therapy with surgical treatment including total hysterectomy and chemotherapy are desirable for patients with metastasis (Grade C1).

CQ48 How should patients with persistent low-positive hCG be treated?

Recommendations:

After every gestation including hydatidiform mole or after treatment of trophoblastic disease, strict follow-up is recommended when 'real' low-unit hCG persists long term without an obvious lesion (Grade C1).

Acknowledgments We thank the Japan Society of Obstetrics and Gynecology, the Japan Association of Obstetricians and Gynecologists, the Japanese Gynecologic Oncology Group, the Japan Society of Clinical Oncology, and the Japanese Society for Therapeutic Radiology and Oncology for their comments and contributions throughout the project. We also acknowledge the support by grants from the Ministry of Health, Labour and Welfare and H24-Clinical Cancer Research-001 (chief researcher, Koichi Hirata).

Members of guidelines formulation committee Yasuhiko Ebina, Hisaya Fujiwara, Shinji Fukunaga, Yasuyuki Hasuo, Atsushi Hongo, Kazuhiko Ino, Yuko Kaneyasu, Hidenori Kato, Naoki Kawamura, Yoichi Kobayashi, Kaneyuki Kubushiro, Masataka Kudo, Hideo Matsui, Koji Matsumoto, Yoshiki Mikami, Toshinari Muramatsu, Shoji Nagao, Satoru Nagase, Takafumi Nakamura, Toru Nakanishi, Satoru Nakayama, Hideyuki Ohtake, Yoshikazu Ozaki, Nobuyuki Susumu, Tsutomu Tabata, Kiyoshi Takamatsu, Masashi Takano, Satoshi Takeuchi, Yoshito Terai, Takafumi Toita, Akiko Tozawa, Takashi Uno, Hidemichi Watari, Tetsuro Yahata, Hideko Yamamoto, Koji Yamazawa, Nozomu Yanaihara, Masami Yasuda, Yoshihito Yokoyama.

Members of guidelines evaluation committee Daisuke Aoki, Yoichi Aoki, Makoto Emoto, Takayuki Enomoto, Toru Hachisuga, Seiryu Kamoi, Takahiro Kasamatsu, Noriyuki Katsumata, Junzo Kigawa, Hiroaki Kobayashi, Takeshi Kodaira, Junichi Kodama, Shinichi Komiyama, Hiroyuki Kuramoto, Makoto Kuroda, Masaki Mandai, Etsuko Miyagi, Takashi Nakano, Kaei Nasu, Fumitaka Numa, Kazunori Ochiai, Tsuyoshi Saito, Toshiaki Saito, Masaru Sakamoto, Noriaki Sakuragi, Nobuhiro Takeshima, Toshimitsu Toya, Satoshi Umezawa, Yoh Watanabe, Hiroyuki Yanai.

Compliance with ethical standards

Conflict of interest Kiyoshi Takamatsu received lecture fees from Bayer Yakuhin, Ldt, and Pfizer Japan Inc.

References

1. Matsuda A, Matsuda T, Shibata A et al (2014) Cancer incidence and incidence rates in Japan in 2008: a study of 25 population-based cancer registries for the Monitoring of Cancer Incidence in Japan (MCIJ) project. Jpn J Clin Oncol 44(4):388–396

2. For act on anti-cancer measures based on the data of statistics white paper 2012 (Shinoharashinsha Publishers Inc.) Cancer Information Service, National Cancer Center, Japan
3. Nagase S, Katabuchi H, Hiura M et al (2010) Evidence-based guidelines for treatment of uterine body neoplasmin Japan: Japan Society of Gynecologic Oncology (JSGO) 2009 edition. Int J Clin Oncol 15:531–542
4. Ariyoshi H (2002) Guideline for correct use of antineoplastic agents (draft). General theory. Gan To Kagaku Ryoho 29(6):970–977 **(in Japanese)**
5. Ochiai K, Okamoto A, Katsumata N (2002) Guidelines for proper use of antineoplastic agents. Gynecologic cancer. Gan To Kagaku Ryoho 29(6):1047–1054 **(in Japanese)**
6. Fukui T, Yoshida M, Yamaguchi N (2007) Minds clinical practice guideline. Igaku-Shoin, Tokyo, p 40 **(in Japanese)**
7. Dowdy SC, Mariani A, Lurain JR (2012) Uterine cancer. In: Berek JS (ed) Berek and Novak's gynecology, 15th edn. Lippincot Williams & Wilkins, Philadelphia, PA, pp 1250–1303
8. Miller DS, Creasman WT (2012) Adenocarcinoma of the uterine corpus. In: DiSaia PJ, Creasman WT (eds) Clinical gynecologic oncology, 8th edn. Elsevier Saunders, Philadelphia, pp 141–174

Clinical Case Reports

Open Access

CASE REPORT

Successful outcome following detection and removal of a very small ovarian teratoma associated with anti-NMDA receptor encephalitis during pregnancy

Etsuko Mizutamari[1], Yuji Matsuo[1], Tomohiro Namimoto[2], Takashi Ohba[1], Yasuyuki Yamashita[2] & Hidetaka Katabuchi[1]

[1]Department of Obstetrics and Gynecology, Faculty of Life Science, Kumamoto University, 1-1-1 Honjo, Chuo-ku, Kumamoto-city, Kumamoto 860-8556, Japan
[2]Department of Diagnostic Radiology, Faculty of Life Science, Kumamoto University, 1-1-1 Honjo, Chuo-ku, Kumamoto-city, Kumamoto 860-8556, Japan

Correspondence
Etsuko Mizutamari, Department of Obstetrics and Gynecology, Faculty of Life Science, Kumamoto University, 1-1-1 Honjo, Chuo-ku, Kumamoto-city, Kumamoto 860-8556, Japan. Tel: +81 96 373 5269; Fax: +81 96 363 5164; E-mail: mizutamarietsuko@gmail.com

Funding Information
No sources of funding were declared for this study.

Received: 9 September 2015; Revised: 16 November 2015; Accepted: 18 November 2015

Clinical Case Reports **2016; 4(3): 223–225**

doi: 10.1002/ccr3.475

Key Clinical Message

An important part of anti–*N*-methyl-D-aspartate (NMDA) receptor encephalitis treatment is prompt detection and removal of any associated ovarian teratoma, regardless of size. High-resolution transvaginal ultrasonography followed by targeted CT with adaptive iterative dose reduction (AIDR) is a useful strategy for distinguishing small ovarian teratomas from luteal cysts during pregnancy.

Keywords

Adaptive iterative dose reduction, anti-NMDA receptor encephalitis, ovarian teratoma, pregnancy, ultrasonography.

Introduction

Anti–*N*-methyl-D-aspartate (NMDA) receptor encephalitis was identified in 2007 by Dalmau and colleagues [1]. It is caused by an autoimmune reaction against the NMDA receptor, which is characterized by psychiatric and neurologic symptoms mimicking herpetic encephalitis. The onset of anti-NMDA receptor encephalitis in females is associated with ovarian teratomas [1, 2]. Herein we report a case of anti-NMDA receptor encephalitis without neurological sequelae after prompt detection and treatment of a small ovarian teratoma in a pregnant woman at 16 weeks of gestation.

Case Report

A healthy 30-year-old gravida 1 para 1 woman conceived naturally and began receiving prenatal care at a local general hospital. She had a history of left ovarian teratoma, which was resected at 24 years of age. During week 15 of gestation, she initially developed a high fever with headaches, and was admitted to the local general hospital. Viral encephalitis was initially suspected but ruled out. Despite symptomatic treatment, her condition worsened. She was referred to Kumamoto University Hospital because of an altered state of consciousness and aspiration pneumonia at 16 weeks +1 day of gestation.

On admission, she had nuchal rigidity and was in respiratory failure requiring mechanical ventilation in the intensive care unit. On hospital day 3, anti-NMDA receptor antibodies were found in her cerebrospinal fluid, prompting us to explore for an ovarian teratoma. Non-contrast magnetic resonance imaging (MRI, MAGNETOM Trio A Tim System 3T, SIEMENS, Erlangen, Germany) detected a cystic mass in the right ovary (Fig. 1A); however, since it was difficult to distinguish

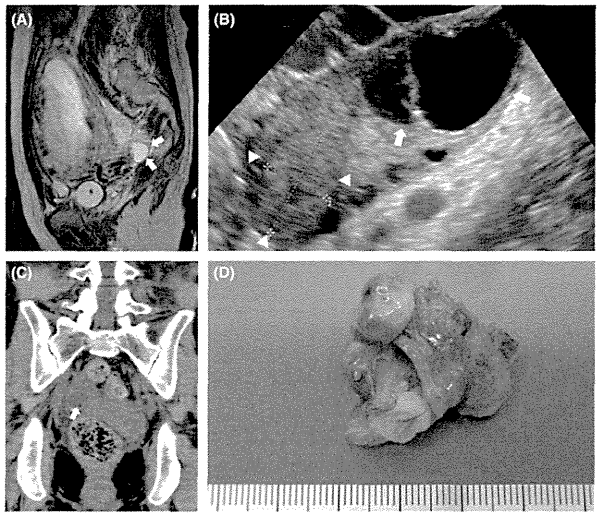

Figure 1. (A) T2-weighed magnetic resonance images of the pelvis in the sagittal plane at 16 weeks of gestation. A cystic mass (arrows) was found in the right adnexa. A lipid component could not be detected. (B) High-resolution transvaginal ultrasonography of the right ovary. A cystic mass (arrows) was detected next to the corpus luteum (arrowheads). (C) Noncontrast computed tomography with adaptive iterative dose reduction of the adnexal area was performed at 16 weeks of gestation. A tiny lipid component (arrow) was detected in the adnexal mass. (D) Macroscopic findings of the right ovarian tumor. The tumor measured 10 × 25 × 30 mm^3 and contained adipose tissue and hair.

this mass from a luteal cyst, we could not confirm the diagnosis of ovarian teratoma. High-resolution transvaginal ultrasonography (RIC6-12-D convex probe, 5.0–13.0 MHz; Voluson E8, GE Healthcare UK, Buckinghamshire, England) detected a cystic mass next to the corpus luteum of the right ovary (Fig. 1B). Noncontrast computed tomography (CT, 120 kV, 150 mA; Aquilion ONE, Toshiba Medical, Tochigi, Japan) with adaptive iterative dose reduction (AIDR) targeting the right adnexa showed that the mass had a very small lipid component (Fig. 1C). The volume CT dose index was 12 mGy, and the dose-length product was 432 mGy/cm. These findings were consistent with ovarian teratoma, and she was scheduled for laparotomy. Right oophorocystectomy was performed at 16 weeks + 4 days of gestation. The tumor measured 10 × 25 × 30 mm^3 (Fig. 1D). Pathological examination revealed mature cystic teratoma of the right ovary. After 4 weeks of postoperative therapy including five courses of plasma exchange, intravenous immunoglobulin therapy, and methylprednisolone pulse therapy, she recovered steadily. She was discharged at 25 weeks of gestation. Subsequently, her pregnancy was uneventful and she delivered a healthy baby at 40 weeks. Anti-NMDA receptor antibody titers were negative in the umbilical vein blood sample. The mother and the infant were healthy with no obvious symptoms.

Discussion

Approximately 90% of patients with anti-NMDA receptor encephalitis are female, and more than 50% of them have ovarian teratoma [3]. Detection and subsequent removal of the teratoma in patients with anti-NMDA receptor encephalitis results in greater clinical improvement than in patients with no detected tumor [4].

It has been suggested that the severity of encephalitis is not related to tumor size [5]. Since anti-NMDA receptor encephalitis often occurs with very small ovarian teratomas and results in serious, irreversible symptoms, evaluation for an ovarian teratoma followed by prompt surgical resection is crucial.

While assessing an ovarian mass during pregnancy, adverse effects on the fetus and differentiating the mass from a luteal cyst are important considerations. Various imaging modalities such as ultrasonography, MRI, and CT are used to evaluate ovarian masses during pregnancy. Although ultrasonography and MRI can be used safely to evaluate adnexal masses during pregnancy, it is difficult

to differentiate ovarian tumors from luteal cysts during early pregnancy. Hoover et al. reported that 17% of ovarian masses that were surgically removed during pregnancy were functional cysts, including corpus luteal cysts [6]. Although CT is a powerful tool for detecting a lipid component, which is characteristic of teratomas, pelvic CT in the first trimester is relatively contraindicated due to possible adverse effects on the developing fetus.

The fetal exposure doses from a single pelvic CT examination remains below the consensus level or levels associated with negligible risk (50–150 mGy), well below the actionable level of 150 mGy [7]. Moreover, AIDR technology has been developed to eliminate noise and artifacts from reduced-dose CT examinations. Image quality and resolution are similar to standard CT, but with significantly lower (38.2%) radiation doses [8]. Compared to standard CT, the radiation dose in our patient was reduced in half by the use of AIDR and targeting the adnexal area. Our case suggests that high-resolution transvaginal ultrasonography followed by targeted reduced-dose CT with AIDR is a useful strategy for distinguishing very small ovarian teratomas from luteal cysts during pregnancy.

In conclusion, appropriate treatment, including prompt detection with transvaginal ultrasonography followed by reduced-dose CT with AIDR and surgical resection of an ovarian teratoma, can result in a good prognosis for both mother and child.

Conflict of Interest

None declared.

References

1. Dalmau, J., E. Tüzün, H. Wu, J. Masjuan, J. E. Rossi, A. Voloschin, et al. 2007. Paraneoplastic anti-N-methyl-D-aspartate receptor encephalitis associated with ovarian teratoma. Ann. Neurol. 61:25–36.
2. Tüzün, E., L. Zhou, J. M. Baehring, S. Bannykh, M. Rosenfeld, and J. Dalmau. 2009. Evidence for antibody-mediated pathogenesis in anti-NMDAR encephalitis associated with ovarian teratoma. Acta Neuropathol. 118:737–743.
3. Dalmau, J., A. J. Gleichman, E. G. Hughes, J. Rossi, X. Peng, M. Lai, et al. 2008. Anti-NMDA receptor encephalitis: case series and analysis of the effects of antibodies. Lancet Neurol. 7:1091–1098.
4. Dalmau, J., E. Lancaster, E. Martinez-Hernandez, M. R. Rosenfeld, and R. Balice-Gordon. 2011. Clinical experience and laboratory investigations in patients with anti-NMDAR encephalitis. Lancet Neurol. 10: 63–74.
5. Motohara, T., S. Tayama, D. Narantuya, H. Tashiro, and H. Katabuchi. 2013. Anti-N-methyl D-aspartate receptor encephalitis associated with ovarian teratoma: clinical presentation, diagnosis, treatment, and surgical management. Int. Cancer Conf. J. 2: 121–130.
6. Hoover, K., and T. R. Jenkins. 2011. Evaluation and management of adnexal mass in pregnancy. Am. J. Obstet. Gynecol. 205:97–102.
7. McCollough, C. H., B. A. Schueler, T. D. Atwell, N. N. Braun, D. M. Regner, D. L. Brown, et al. 2007. Radiation exposure and pregnancy: when should we be concerned? Radiographics 27:909–918.
8. Gonzalez-Guindalini, F. D., M. P. F. Botelho, H. G. Töre, R. W. Ahn, L. I. Gordon, and V. Yaghmai. 2013. MDCT of chest, abdomen, and pelvis using attenuation-based automated tube voltage selection in combination with iterative reconstruction: an intrapatient study of radiation dose and image quality. Am. J. Roentgenol. 201: 1075–1082.

Cancer Science
Japanese Cancer Association JCA
Open Access

Prognostic significance of CD169-positive lymph node sinus macrophages in patients with endometrial carcinoma

Koji Ohnishi,[1,4] Munekage Yamaguchi,[2,4] Chimeddulam Erdenebaatar,[2] Fumitaka Saito,[2] Hironori Tashiro,[3] Hidetaka Katabuchi,[2] Motohiro Takeya[1] and Yoshihiro Komohara[1]

Departments of [1]Cell Pathology; [2]Obstetrics and Gynecology, Graduate School of Medical Sciences, Faculty of Life Sciences, Kumamoto University, Kumamoto; [3]Department of Mother-Child Nursing, Faculty of Life Sciences, Kumamoto University, Kumamoto, Japan

Key words

CD169, endometrial carcinoma, NK cell, regional lymph node, sinus macrophage

Correspondence

Yoshihiro Komohara, Department of Cell Pathology, Graduate School of Medical Sciences, Kumamoto University, 1-1-1 Honjo, Chuo-ku, Kumamoto 860-8556, Japan.
Tel: 81-96-373-5095; Fax: 81-96-373-5095;
E-mail: ycomo@kumamoto-u.ac.jp

[4]These authors contributed equally to this work.

Funding Information

Grants-in-Aid for Scientific Research from the Ministry of Education, Culture, Sports, Science, and Technology of Japan (25293089 and 26460454).

Received October 22, 2015; Revised March 7, 2016; Accepted March 13, 2016

Cancer Sci (2016)

doi: 10.1111/cas.12929

Lymph node (LN) macrophages play critical roles in anti-tumor immunity, which develops via the activation of cytotoxic T cells (CTL) and NK cells. The present study aims to determine the prognostic significance of CD169$^+$ LN macrophages in patients with endometrial carcinoma (EC). The number of CD169$^+$ cells or the CD169$^+$-to-CD68$^+$ macrophage ratio in regional LN (RLN), and the number of CD8$^+$ CTL or CD57$^+$ NK cells in tumor tissues were investigated by immunohistochemistry in paraffin-embedded tissue samples from 79 patients with EC. A high density of CD169$^+$ cells in the RLN of patients with EC was correlated with an early clinical stage or no LN metastasis. A high number of CD169$^+$ cells and a high CD169$^+$-to-CD68$^+$ macrophage ratio were significantly associated with longer overall survival in EC. We also found that the density of CD169$^+$ macrophages was positively correlated with the number of CD8$^+$ CTL and CD57$^+$ NK cells that infiltrated into tumor tissues. A high density of CD57$^+$ cells in EC tissues was associated with a better prognosis, while a high density of CD8$^+$ cells was not linked to an altered prognosis. The present study showed that the density of CD169$^+$ macrophages in RLN was associated with an improved prognosis in EC patients. CD169$^+$ macrophages in RLN might represent a useful marker for assessing clinical prognoses and monitoring anti-tumor immunity in patients with EC.

Lymph nodes (LN) are one of the initial organs that dominate immune responses to immunogenic antigens, such as those derived from pathogens or tumor cells. In the case of antitumor immunity, regional lymph nodes (RLN) that drain various malignant tumors are thought to be the first site where the immune system makes contact with tumor cells or their products.[1] Fragmented dead tumor cells can flow into the sinus area of the RLN via lymphatic vessels and then can be endocytosed by a specialized type of resident macrophage, known as sinus macrophages.[2] Sinus macrophages internalize, process and present antigens on MHC I complexes, and induce activation of tumor antigen-specific T-cell and B-cell responses.[3,4] These findings may indicate that the actions of sinus macrophages in RLN represent a critical component of the antitumor immune response.

Sinus macrophages in the LN specifically express CD169, a transmembrane receptor that is also known as sialoadhesin or sialic acid-binding lectin (Siglec)-1.[5,6] CD169 binds sialylated glycoproteins, including CD43 (sialophorin) and MUC1, and is involved in mediating both cell–cell adhesion and cell–pathogen interactions.[6–8] CD169 is also involved in hematopoiesis and the activation of B, T and NK cells.[6,9] Previous studies of CD169-deficient mice suggested that CD169 might exacerbate disease in experimental autoimmune encephalomyelitis by inhibiting regulatory T-cell accumulation.[10] In other studies, CD169$^+$ liver macrophages have been shown to promote the cluster formation and the subsequent activation of both CD4$^+$ and CD8$^+$ T cells.[11] CD169$^+$ sinus macrophages can also activate NK cells by responding to lymph-borne viral particles.[12] These findings suggest that CD169$^+$ macrophages have proinflammatory functions related to T-cell and NK cell activation.

Endometrial cancer (EC) is the most common malignant gynecological disease, with an incidence of approximately 287 000 new cases per year, and represents the sixth most common cancer in women worldwide.[13,14] Recently, the incidence rates of EC have continually increased. Most patients with early-stage EC have an excellent outcome because of effective treatment options, including total hysterectomy and bilateral salpingo-oophorectomy with systematic pelvic/para-aortic lymphadenectomy. High-grade EC, however, show a poor prognosis, despite performing adjuvant therapies that include radiotherapy and chemotherapy. Therefore, alternative therapeutic strategies, such as immunotherapy, are thought to be necessary.[15] EC with a high density of intratumoral CD8$^+$ T-cell infiltration have been established to show a favorable prognosis.[16–18] Clinical trials of immunotherapies targeting several tumor antigens, such as Wilms' tumor gene 1 (WT1)[19] and survivin,[20] have been performed in patients with EC. For example, three out of four

Human Leucocyte Antigen-A2-positive EC patients showed tumor regression based on vaccination of autologous dendritic cells electroporated with WT1 mRNA.[20] Together, these findings indicate that enhancing the anti-tumor activity of $CD8^+$ cytotoxic T cells and/or NK cells represents an attractive potential therapy for various malignancies.

Asano and colleagues found that $CD169^+$ LN macrophages could engulf tumor cell antigens and provoke the proliferation of antigen-specific $CD8^+$ cytotoxic T cells in a mouse tumor transplantation model.[21] Bernhard and colleagues show that $CD169^+$ LN macrophages could induce antigen-specific cytotoxic T-cell responses in dendritic cell-depleted mice.[22] Together, these findings suggest that $CD169^+$ macrophages play an important role in tumor antigen-targeted immunotherapy by presenting tumor antigens to cytotoxic lymphocytes. However, interactions between $CD169^+$ macrophages and anti-tumor immune responses in human EC patients have not yet been fully addressed. Therefore, we investigated potential correlations between $CD169^+$ RLN macrophages and infiltrating immune cells by immunohistochemistry using pathological specimens that we obtained from patients with EC.

Materials and Methods

Patients. In this study, paraffin-embedded specimens of primary lesions and RLN resected from 79 patients with EC who had undergone surgery at Kumamoto University Hospital between 2003 and 2007 were used. Patient characteristics are indicated in Table S1. The right obturator or internal iliac lymph nodes were dissected as RLN. All patients provided informed written consent for participation in this study, in accordance with protocols approved by the Kumamoto University Hospital Review Board.

Immunostaining and double immunostaining. Tissue samples from EC lesions or RLN were routinely fixed in 10% neutral buffered formalin and embedded in paraffin. All 3-μm serial sections were stored in a deep freezer until immunostaining was performed. Antigen retrieval was performed as follows: sections were immersed in 1-mM ethylenediamine tetra-acetic acid solution (pH 8.0), and samples were heated in a microwave (95°C, 5 min) for CD169 staining (clone HSn 7D2; Santa Cruz Biotechnology, Santa Cruz, CA, USA) or using a pressure cooker for staining CD68 (clone PG-M1; Dako, Glostrup, Denmark), CD57 (clone NK-1; Leica, Wetzlar, Germany) and CD8 (clone C8/144B; Nichirei, Tokyo, Japan). An isotype-matched mouse IgG (Dako) antibody was used as a negative control. Following incubation with primary antibodies, samples were incubated with an HRP-labeled goat anti-mouse antibody (Nichirei). Immune reactivity was visualized using a diaminobenzidine substrate system (Nichirei). Double immunostaining of CD169 and CD57 in RLN was performed as described previously.[23] Briefly, sections were incubated with an anti-CD57 antibody, staining was visualized using DAB, and then slides were washed with citrate buffer (pH 2.2). Sections were then incubated with anti-CD169 antibodies and visualized using HistoGreen (Linaris, Dossenheim, Germany).

Macrophages counts in regional lymph nodes and assessments of $CD8^+$ T-cell and $CD57^+$ NK cell infiltration in primary lesions. It

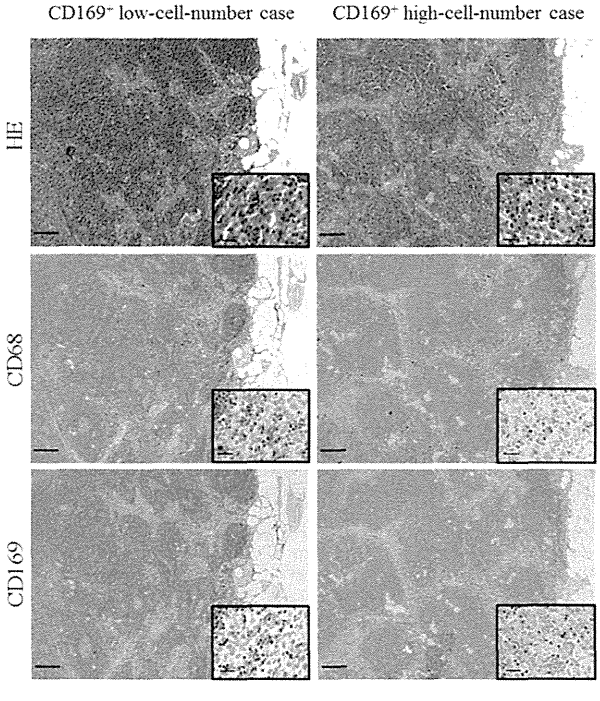

Fig. 1. Immunostaining of sinus macrophages in the regional lymph node (RLN) of the endometrial carcinoma (EC) patients. HE staining of sinus areas in the RLN and immunohistochemical analyses of $CD68^+$ and $CD169^+$ macrophages in the RLN. Representative results are shown for cases with high or low numbers of $CD169^+$ cells. Higher magnification images of the squared area are inserted in the lower right inset. Scale bar, 50 μm.

Table 1. Clinicopathological features and the number of macrophages in regional lymph nodes (RLN) from 79 patients with endometrial carcinoma (EC)

Clinicopathological feature	*n*	$CD169^+$ cells/mm^2 in RLN			$CD68^+$ cells/mm^2 in RLN		
		<350	≥350	*P*-value	<750	≥750	*P*-value
Age (years)							
<60	41	20	21	NS	17	24	NS
≥60	38	19	19		22	16	
Stage							
I	41	21	30	0.049*	25	26	NS
II–IV	38	18	10		14	14	
Grading							
G1	27	12	15	NS	11	16	NS
G2, 3	44	24	20		25	19	
Depth of muscle invasion							
<50%	46	21	25	NS	21	25	NS
≥50%	28	13	15		13	15	
Vascular invasion							
Negative	40	18	22	NS	20	20	NS
Positive	33	17	16		18	15	
Lymph node metastasis							
Negative	66	29	37	0.029*	32	34	NS
Positive	13	10	3		7	6	
Menstruation							
Premenopausal	23	8	15	NS	5	18	NS
Postmenopausal	56	26	30		25	31	
$CD8^+$ cells/mm^2 in tumor							
<120	36	20	16	NS	21	15	NS
≥120	39	17	22		17	22	
$CD57^+$ cells/mm^2 in tumor							
<50	38	25	13	0.004*	21	17	NS
≥50	37	12	25		17	20	

*Statistically significant results. NS, not significant.

was possible to identify RLN sinus areas visually on H&E-stained slides because sinus areas are clearly demarcated by reticular fibers. The numbers of $CD68^+$ and $CD169^+$ cells per mm^2 in sinus areas in RLN without metastatic cancer cells and the numbers of $CD8^+$ and $CD57^+$ cells per mm^2 in intra-tumor areas were counted in high power fields (0.028 mm^2 per field) by two independent pathologists (K.O. and Y.K.). Both pathologists were blinded to the identities of the samples. To calculate the number of positive cells per unit area, we measured the areas (mm^2) using the ImageJ software program (US National Institute of Health, Bethesda, MD, USA). Count data assessed by K.O. or Y.K. were averaged as described previously.[23]

Statistical analysis. Statistical analyses were carried out using JMP 10 (SAS Institute, Chicago, IL, USA). Associations between different categorical variables were assessed using multivariate analysis. The cumulative survival rate was compared between two groups via the log-rank test and generalized using the Wilcoxon test. Simultaneous relationships between multiple prognostic factors for survival were assessed using the Cox proportional hazards model with stepwise backwards reductions. Multivariate analysis included adjustments for age, clinical stages, histological grades, LN metastasis, the ratio of $CD169^+$-to-$CD68^+$ cells in RLN, and the number of $CD57^+$ cells in tumor tissue. A *P*-value < 0.05 was considered to represent a statistically significant difference.

Table 2. Univariate and multivariate Cox regression analyses of potential prognostic factors for overall survival in patients with endometrial carcinoma (EC) (*n* = 79)

Clinicopathological feature	*n*	Univariate analysis *P*-value		Multivariate analysis		
		Log-rank	Wilcoxon	HR	95% CI	*P*-value
Age (years)						
<60	41	0.0393*	0.0431*	8.08	0.01–0.12	<0.001*
≥60	38					
Stage						
I	41	0.0016*	0.0012*	ND	ND	ND
II–IV	38					
Grading						
G1	27	0.0235*	0.0229*	4.46	1.59–14.42	0.0036*
G2, 3	44					
Depth of muscle invasion						
<50%	46	0.1435	0.1185	ND	ND	ND
≥50%	28					
Vascular invasion						
Negative	40	0.2808	0.3001	ND	ND	ND
Positive	33					
Lymph node metastasis						
Negative	66	0.0028*	0.0029*	3.99	1.52–10.8	0.0054*
Positive	13					
Menstruation						
Premenopausal	23	0.7004	0.6791	ND	ND	ND
Postmenopausal	56					
$CD169^+$ cells/mm^2 in RLNs						
<350	40	0.0139*	0.0098*	ND	ND	ND
≥350	39					
$CD68^+$ cells/mm^2 in RLNs						
<750	40	0.6403	0.5173	ND	ND	ND
≥750	39					
$CD169^+$ cells/$CD68^+$ cells in RLNs						
<0.7	41	0.0042*	0.0029*	1.29	0.72–2.39	0.395
≥0.7	38					
$CD8^+$ cells/mm^2 in tumor						
<120	36	0.0959	0.1098	ND	ND	ND
≥120	39					
$CD57^+$ cells/mm^2 in tumor						
<50	38	0.0114*	0.0177*	0.32	0.11–0.83	0.018*
≥50	37					

*Statistically significant results. CI, confidence interval; HR, hazard ratio; ND, not done.

Results

Fewer $CD169^+$ sinus macrophages in regional lymph node from endometrial carcinoma patients with advanced-stage or lymph node metastasis. We first performed immunostaining to investigate CD68 and CD169 expression in RLN obtained from all EC patients. In patients with LN metastasis, RLN that contained no metastatic carcinoma cells were used for these evaluations. The RLN sinus could be clearly identified as a demarcated area filled with macrophages by both H&E staining and immunostaining. All sinus macrophages were positive for the pan-macrophage marker CD68, while the number of $CD169^+$ sinus macrophages varied in each patient (Fig. 1). In addition, the sinus macrophages around metastatic carcinoma cells were completely negative for CD169 in RLN of patients

with LN metastasis. Similar results were found in other pelvic RLN such as iliac, inguinal or sacral LN (Table S2).

We then analyzed correlations between the clinicopathological features and the number of sinus macrophages in patients with EC. We counted $CD68^+$ and $CD169^+$ cells in the sinus areas, and subsequently classified patients into two groups (those with a low or high cell number) based on the adequate cut-off value, which was selected by using a comparable categorization while referring to the median count. Statistical analyses showed that fewer $CD169^+$ cells and a lower ratio of $CD169^+$-to-$CD68^+$ macrophages were strongly correlated with an advanced clinical stage or LN metastasis; however, the number of $CD169^+$ cells per mm^2 and ratio of $CD169^+$-to-$CD68^+$ macrophages were not associated with age, grading, depth of muscle invasion, vascular invasion or menstruation (Table 1).

Association of a high density of $CD169^+$ sinus macrophages with a good prognosis in endometrial carcinoma patients. The number of $CD169^+$ cells per mm^2 and the ratio of $CD169^+$-to-$CD68^+$ macrophages were significantly correlated with more favorable overall survival in a univariate analysis (log-rank test, $P = 0.0139$ and $P = 0.0042$, respectively), but our multivariate analysis indicated that there was no significant correlation (Table 2, Fig. 2). In addition, no correlation existed between the number of $CD68^+$ RLN macrophages and overall survival (Fig. 2). A younger age (<60 years), a lower clinical stage (stage 1), a low histological grading (grade 1) and the absence of LN metastasis were also associated with longer overall survival in the univariate analysis (Table 2). Multivariate analysis showed a significant correlation between overall survival and age, grading, and LN status (Table 2).

Density of $CD169^+$ sinus macrophages correlated positively with $CD8^+$ T-cell or $CD57^+$ NK cell infiltration in tumor tissues. We next analyzed potential associations between $CD169^+$ RLN macrophages and tumor-infiltrating $CD8^+$ T cells or $CD57^+$ NK cells in tissues from EC patients. The number of both $CD8^+$ T cells and $CD57^+$ NK cells in tumor nests and tumor stroma increased significantly when $CD169^+$ RLN sinus macrophages were abundant (Fig. 3a). The number of $CD169^+$ cells and the ratio of $CD169^+$-to-$CD68^+$ cells correlated positively with the number of $CD8^+$ T cells or $CD57^+$ NK cells in tumor nests and tumor stroma (Fig. 3b). EC patients with abundant $CD57^+$ NK cell infiltration had a more favorable overall survival; however, the number of $CD8^+$ T cells in tumor tissue was not associated with overall survival in EC patients (Table 2, Fig. 3c).

Although $CD169^+$ sinus macrophages exhibited direct contact with $CD8^+$ T cells that expressed CD43, a major ligand of CD169, in the sinus area of RLN in colorectal cancer patients,[2,3] whether interactions occur between $CD169^+$ sinus macrophages and $CD57^+$ NK cells in RLN has remained unclear. To investigate the details of interactions between macrophages and NK cells in RLN, we performed double immunostaining using monoclonal antibodies for CD169 and CD57. We found that approximately 10% of $CD169^+$ cells made direct contact with $CD57^+$ NK cells in the sinus area of the RLN (Fig. 3d).

Discussion

In this present study, we observed greater numbers of $CD169^+$ cells and ratios of $CD169^+$-to-$CD68^+$ macrophages in cases of EC with an early clinical stage or no LN metastasis; these findings were significantly correlated with a more favorable overall survival of EC patients. The significant correlation between the number of $CD169^+$ sinus macrophages and density of infiltrating $CD8^+$ T cells and $CD57^+$ NK cells in the primary lesions suggests that $CD169^+$ RLN macrophages are closely associated with the activation of cytotoxic lymphocyte-mediated antitumor immunity.

Although many previous studies of $CD169^+$ macrophages had led to advances in understanding the distribution of these cells

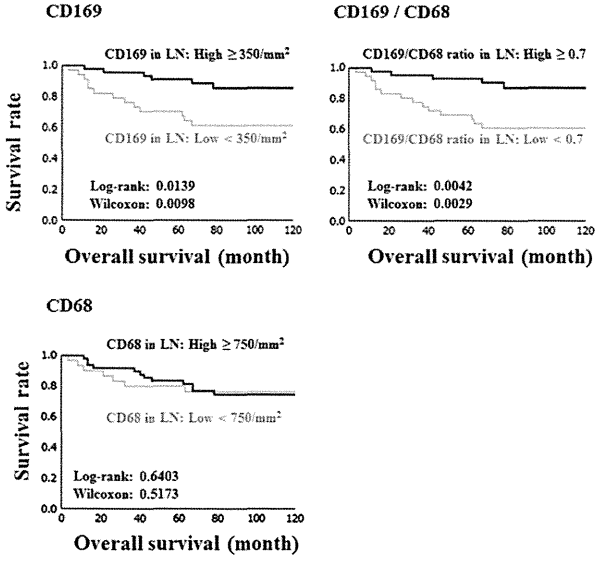

Fig. 2. Overall, Kaplan–Meier survival curves for 79 endometrial carcinoma (EC) patients as related to the number of $CD169^+$ macrophages, $CD169^+$-to-$CD68^+$ macrophage ratio, and number of $CD68^+$ macrophages in regional lymph node (RLN). LN, lymph node.

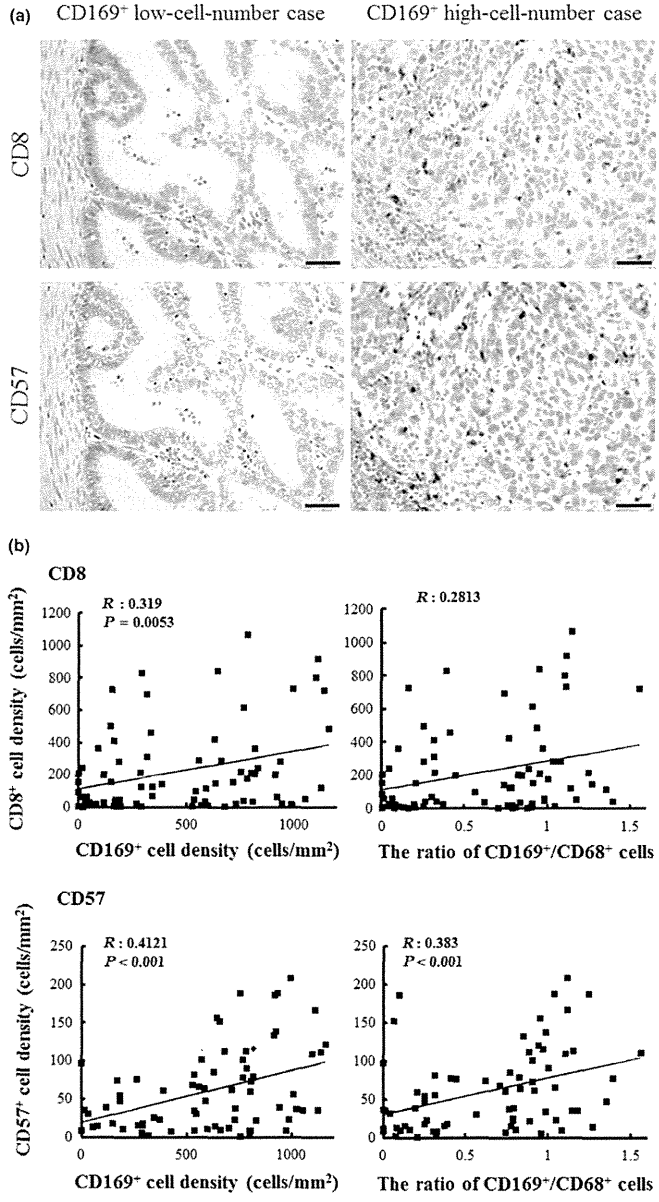

Fig. 3. Interactions between CD169⁺ macrophages in the regional lymph node (RLN) and CD8⁺ T cells or CD57⁺ NK cells in endometrial carcinoma (EC). (a) Immunohistochemical analyses of CD8⁺ T cells and CD57⁺ NK cells in tumor tissues. Scale bar, 50 μm. (b) Correlation between the number of CD8⁺ T cells or CD57⁺ NK cells in tumor tissues and the number of CD169⁺ macrophages or the CD169⁺-to-CD68⁺ macrophage ratio in RLN. (c) Overall survival curves for patients showing CD8⁺ T cells or CD57⁺ NK cells in tumor tissues. (d) Double immunostaining of CD169 and CD57 in RLN. Arrowheads indicate direct contacts between CD169⁺ cells and CD57⁺ cells. Scale bar, 50 μm.

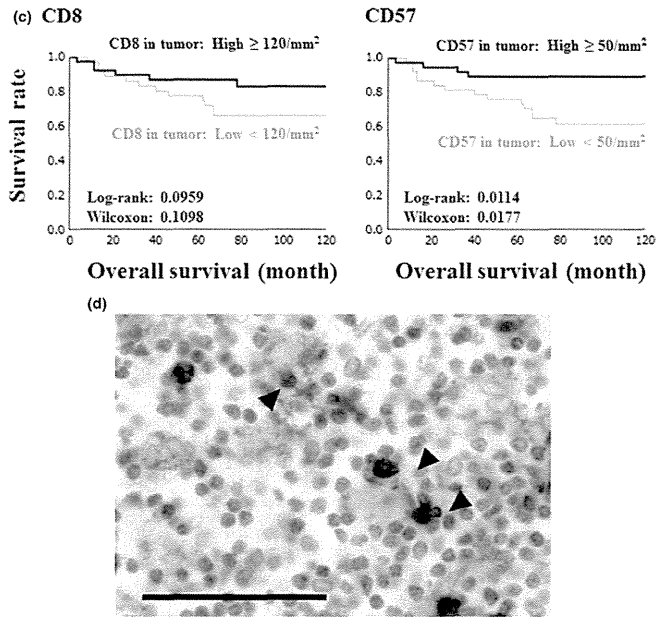

Fig. 3. Continued

among various macrophage subsets in rodents, only a few have described the regulation of CD169 expression in human macrophages.[5,6] Previously, we showed that a high number of CD169$^+$ sinus macrophages were closely associated with a better prognosis and a higher density of infiltrating CD8$^+$ T cells in tumors of patients with colorectal carcinomas or melanomas.[23,24] Although the density of CD169$^+$ macrophages in RLN was not an independent risk factor for overall survival by multivariate analysis, a higher number of CD169$^+$ macrophages and an increased ratio of CD169$^+$-to-CD68$^+$ macrophages in RLN were both significantly associated with a better clinical prognosis in patients with EC. Moreover, we found that the density of CD169$^+$ macrophages was positively correlated with the number of CD8$^+$ T cells and CD57$^+$ NK cells in tumor tissues. These findings suggest that CD169$^+$ sinus macrophages might activate cytotoxic lymphocyte-mediated anti-tumor immunity in EC.

Generally, NK cells are considered to be important for immune responses to malignant tumors in humans. Previous studies have examined associations between NK cell infiltration into tumors in patients with breast cancer,[25] vulvar cancer[26] and colorectal cancer,[27,28] and renal cell carcinoma;[29] however, the significance of NK cells in patients with EC had not yet been reported. The present study reveals that EC cases with abundant NK cell infiltration showed better overall survival. Moreover, the number of CD57$^+$ NK cells in tumor tissues was an independent risk factor for overall survival. Garcia and colleagues showed that CD169$^+$ macrophages promoted the accumulation and activation of NK cells after they engulfed viral particles.[12] Coombes and colleagues demonstrated that CD169$^+$ sinus macrophages which have inflammatory functions are necessary to NK cell activation in the lymph node sinus area.[30] Therefore, we decided to investigate the relationship between CD169$^+$ sinus macrophages and NK cells. By immunohistochemistry, we demonstrated that CD169$^+$ macrophages made direct contact with CD57$^+$ NK cells in the sinus areas of RLN, and that a higher density of CD169$^+$ RLN sinus macrophages was correlated with increased numbers of infiltrating NK cells in tumor tissues. Because all infiltrating macrophages in tumor tissue were negative for CD169 (data not shown), the interaction between CD169$^+$ macrophages and NK cells was shown not in local tumor tissue but in lymph nodes. Although the full mechanism underlying CD169$^+$ macrophage-mediated NK cell activation remains unclear, our findings suggest that CD169$^+$ macrophages play important roles in anti-tumor immunity in patients with EC by activating NK cells.

Our previous and present studies together show that the number of CD169$^+$ sinus macrophages in human LN varies considerably, although the number of total sinus macrophages remains approximately constant. However, the reason for this variation in CD169 expression has remained obscure. In the present study, we chose to but examine LN sinus macrophages that were limited to the right obturator or internal iliac LN, we note that we obtained similar data from other RLN, such as the iliac or sacral LN (Table S2), suggesting that CD169 expression varied systemically rather than focally. We propose the following two potential mechanisms for the regulation of CD169 expression: (i) CD169 expression is different between individuals; and (ii) yet to be characterized lymph-borne effector molecules from tumors suppress CD169 expression. As one potential mechanism, an IFN-α secretion by cells in RLN might be a strong regulator of CD169 expression, as IFN-α-secreting cells are in close proximity to CD169$^+$ sinus

macrophages in the RLN and IFN-α can induce robust CD169 expression in human macrophages.[23,24] Further experiments will be needed to more completely elucidate the mechanisms that regulate CD169 expression in human LN. With a previous paper describing that an activation of NK cells could be enhanced by an IFN-α secretion in the LN sinus area,[12] the $CD169^+$ macrophage-mediated NK cell activation also might be regulated by IFN-α-secreting cells.

In conclusion, we have demonstrated the prognostic significance of $CD169^+$ sinus macrophages in the RLN of patients with EC. A greater number of $CD169^+$ macrophages and an increased ratio of $CD169^+$-to-$CD68^+$ macrophages in the RLN were significantly associated with a better clinical prognosis. $CD169^+$ sinus macrophages found in RLN may, therefore, be involved in cytotoxic T-cell-mediated and NK cell-mediated antitumor immunity. Evaluation of CD169 protein expression in RLN may aid estimations of clinical prognoses and improve the monitoring of anti-tumor immune responses in patients with EC.

Acknowledgments

We sincerely thank Ms Yui Hayashida, Mr Osamu Nakamura and Mr Takenobu Nakagawa for providing valuable technical assistance. The present study was supported in part by Grants-in-Aid for Scientific Research (25293089 and 26460454) from the Ministry of Education, Culture, Sports, Science, and Technology of Japan.

Disclosure Statement

The authors have no conflict of interest to declare.

References

1 Lores B, García-Estevez JM, Arias C. Lymph nodes and human tumors (review). *Int J Mol Med* 1998; **1**: 729–33.
2 Swartz MA. Immunomodulatory roles of lymphatic vessels in cancer progression. *Cancer Immunol Res* 2014; **2**: 701–7.
3 Hickok DF, Miller L, Harris L. Regional hyperplastic lymph nodes in breast cancer: the role of lymphocytes and nodal macrophages. An immunological study with a five-year follow-up. *Surgery* 1977; **82**: 710–5.
4 Gray EE, Cyster JG. Lymph node macrophages. *J Innate Immun* 2012; **4**: 424–36.
5 Martens JH, Kzhyshkowska J, Falkowski-Hansen M, *et al.* Differential expression of a gene signature for scavenger/lectin receptors by endothelial cells and macrophages in human lymph node sinuses, the primary sites of regional metastasis. *J Pathol* 2006; **208**: 574–89.
6 Martinez-Pomares L, Gordon S. CD169+ macrophages at the crossroads of antigen presentation. *Trends Immunol* 2012; **33**: 66–70.
7 Nath D, Hartnell A, Happerfield L, *et al.* Macrophage-tumour cell interactions: identification of MUC1 on breast cancer cells as a potential counter-receptor for the macrophage-restricted receptor, sialoadhesin. *Immunology* 1999; **98**: 213–9.
8 van den Berg TK, Nath D, Ziltener HJ *et al.* Cutting edge: CD43 functions as a T cell counterreceptor for the macrophage adhesion receptor sialoadhesin (Siglec-1). *J Immunol* 2001; **166**: 3637–40.
9 Chow A, Lucas D, Hidalgo A, *et al.* Bone marrow CD169+ macrophages promote the retention of hematopoietic stem and progenitor cells in the mesenchymal stem cell niche. *J Exp Med* 2011; **208**: 261–71.
10 Wu C, Rauch U, Korpos E *et al.* Sialoadhesin-positive macrophages bind regulatory T cells, negatively controlling their expansion and autoimmune disease progression. *J Immunol* 2009; **182**: 6508–16.
11 Müerköster S, Rocha M, Crocker PR, Schirrmacher V, Umansky V. Sialoadhesin-positive host macrophages play an essential role in graft-versus-leukemia reactivity in mice. *Blood* 1999; **93**: 4375–86.
12 Garcia Z, Lemaitre F, van Rooijen N, *et al.* Subcapsular sinus macrophages promote NK cell accumulation and activation in response to lymph-borne viral particles. *Blood* 2012; **120**: 4744–50.
13 Murali R, Soslow RA, Weigelt B. Classification of endometrial carcinoma: more than two types. *Lancet Oncol* 2014; **15**: e268–78.
14 Kübler K, Ayub TH, Weber SK, *et al.* Prognostic significance of tumor-associated macrophages in endometrial adenocarcinoma. *Gynecol Oncol* 2014; **135**: 176–83.
15 Elit L, Hirte H. Current status and future innovations of hormonal agents, chemotherapy and investigational agents in endometrial cancer. *Curr Opin Obstet Gynecol* 2002; **14**: 67–73.
16 Kondratiev S, Sabo E, Yakirevich E, Lavie O, Resnick MB. Intratumoral CD8+ T lymphocytes as a prognostic factor of survival in endometrial carcinoma. *Clin Cancer Res* 2004; **10**: 4450–6.
17 de Jong RA, Leffers N, Boezen HM, *et al.* Presence of tumor-infiltrating lymphocytes is an independent prognostic factor in type I and II endometrial cancer. *Gynecol Oncol* 2009; **114**: 105–10.
18 de Jong RA, Boerma A, Boezen HM, Mourits MJ, Hollema H, Nijman HW. Loss of HLA class I and mismatch repair protein expression in sporadic endometrioid endometrial carcinomas. *Int J Cancer* 2012; **131**: 1828–36.
19 Coosemans A, Vanderstraeten A, Tuyaerts S, *et al.* Wilms' Tumor Gene 1 (WT1)–loaded dendritic cell immunotherapy in patients with uterine tumors: a phase I/II clinical trial. *Anticancer Res* 2013; **33**: 5495–500.
20 Vanderstraeten A, Everaert T, Van Bree R, *et al.* In vitro validation of survivin as target tumor-associated antigen for immunotherapy in uterine cancer. *J Immunother* 2015; **38**: 239–49.
21 Asano K, Nabeyama A, Miyake Y, *et al.* CD169-positive macrophages dominate antitumor immunity by crosspresenting dead cell-associated antigens. *Immunity* 2011; **34**: 85–95.
22 Bernhard CA, Ried C, Kochanek S, Brocker T. CD169+ macrophages are sufficient for priming of CTLs with specificities left out by cross-priming dendritic cells. *Proc Natl Acad Sci USA* 2015; **112**: 5461–6.
23 Ohnishi K, Komohara Y, Saito Y, *et al.* CD169-positive macrophages in regional lymph nodes are associated with a favorable prognosis in patients with colorectal carcinoma. *Cancer Sci* 2013; **104**: 1237–44.
24 Saito Y, Ohnishi K, Miyashita A, *et al.* Prognostic significance of CD169+ lymph node sinus macrophages in patients with malignant melanoma. *Cancer Immunol Res* 2015; **3**: 1356–63.
25 Rathore AS, Goel MM, Makker A, Kumar S, Srivastava AN. Is the tumor infiltrating natural killer cell (NK-TILs) count in infiltrating ductal carcinoma of breast prognostically significant? *Asian Pac J Cancer Prev* 2014; **15**: 3757–61.
26 Sznurkowski JJ, Zawrocki A, Biernat W. Subtypes of cytotoxic lymphocytes and natural killer cells infiltrating cancer nests correlate with prognosis in patients with vulvar squamous cell carcinoma. *Cancer Immunol Immunother* 2014; **63**: 297–303.
27 Qiu H, Xiao-Jun W, Zhi-Wei Z, *et al.* The prognostic significance of peripheral T-lymphocyte subsets and natural killer cells in patients with colorectal cancer. *Hepatogastroenterology* 2009; **56**: 1310–5.
28 Sconocchia G, Eppenberger S, Spagnoli GC, *et al.* NK cells and T cells cooperate during the clinical course of colorectal cancer. *Oncoimmunology* 2014; **3**: e952197.
29 Geissler K, Fornara P, Lautenschläger C, Holzhausen HJ, Seliger B, Riemann D. Immune signature of tumor infiltrating immune cells in renal cancer. *Oncoimmunology* 2015; **4**: e985082.
30 Coombes JL, Han SJ, van Rooijen N, Raulet DH, Robey EA. Infection-induced regulation of natural killer cells by macrophages and collagen at the lymph node subcapsular sinus. *Cell Rep* 2012; **2**: 124–35.

Supporting Information

Additional Supporting Information may be found online in the supporting information tab for this article:

Table S1. Summary of patient characteristics.

Table S2. Distribution of CD169+ cells in dissected regional lymph nodes.

Gynecologic Oncology Reports 14 (2015) 31–33

Contents lists available at ScienceDirect

Gynecologic Oncology Reports

journal homepage: www.elsevier.com/locate/gore

Case report

Choriocarcinoma coexisting with epithelioid trophoblastic tumor of the uterine horn

Yuko Imamura [a], Hironori Tashiro [b,*], Fumitaka Saito [a], Kiyomi Takaishi [a], Takashi Ohba [a], Masaharu Fukunaga [c], Hidetaka Katabuchi [a]

[a] Department of Obstetrics and Gynecology, Faculty of Life Sciences, Kumamoto University, Honjo 1-1-1, Chuo-ku, Kumamoto City, Kumamoto 860-8556, Japan
[b] Department of Mother-Child Nursing, Faculty of Life Sciences, Kumamoto University, Kuhonji 4-24-1, Chuo-ku, Kumamoto City, Kumamoto 862-0976, Japan
[c] Department of Pathology, The Jikei University Daisan Hospital, Izumi Honcho 4-11-1, Komae City, Tokyo 201-8601, Japan

1. Introduction

Clinicopathological studies have provided some evidence regarding the pathogenesis of at least three distinct types of gestational trophoblastic neoplasia (GTN), including the most common type, choriocarcinoma, and two less common ones, placental site trophoblastic tumor (PSTT) and epithelioid trophoblastic tumor (ETT). Choriocarcinoma is composed of variable proportions of neoplastic cytotrophoblast, syncytiotrophoblast, and intermediate trophoblast, the latter of which is composed of a similar mixture of trophoblastic subpopulations. While the neoplastic cytotrophoblast in PSTT differentiates mainly into intermediate trophoblastic cells at the implantation site, the neoplastic cytotrophoblast in ETT differentiates into chorionic-type intermediate trophoblastic cells in the chorion laeve. However, the pathogenesis of the differentiation of GTN, especially ETT, is still unknown because these tumors are extremely rare. Furthermore, there is little evidence regarding therapeutic strategies for GTN, including ETT. Here we present a case of mixed choriocarcinoma coexisting with an ETT, which might elucidate the pathogenesis of ETT and identify an appropriate treatment approach for mixed-type GTN.

2. Case report

A 32-year-old Japanese woman, gravida 2, para 1, visited a previous hospital complaining of secondary amenorrhea. Her medical history was notable for treatment with systemic chemotherapy with methotrexate (MTX) at age 26 for an invasive hydatidiform mole that had developed from a complete mole; she had an uncomplicated full-term delivery 2 years later. Pelvic examination revealed no abnormal findings. Her serum human chorionic gonadotropin (hCG) level was 93,820 mIU/ml. Transvaginal ultrasonography showed a mass in the left uterine horn without a gestational sac. She was first diagnosed with an ectopic pregnancy in the interstitial part of the fallopian tube. Laparoscopic surgery was performed, resulting in the resection of a 2.0-cm mass in the uterine horn. She was monitored closely via serum hCG levels; while these levels decreased postoperatively, they increased again 4 weeks later. The presence of residual chorionic villi was suspected, and she was treated with single-agent chemotherapy with intramuscular MTX 1 mg/kg per day on days 1, 3, 5 and 7 with intramuscular folinic acid 0.1 mg/kg per day on days 2, 4, 6 and 8 every 2 weeks. After a transient decrease, her serum hCG levels again increased at the 5th cycle of chemotherapy. The patient was referred to Kumamoto University Hospital due to the possible diagnosis of gestational trophoblastic disease. Transvaginal Doppler ultrasound examination showed extensive vascularization within the myometrium (Fig. 1, A). Pelvic magnetic resonance imaging demonstrated a high-signal-intensity focus in the myometrium on T2-weighted images. Evaluation by positron emission tomography/computed tomography (PET/CT) revealed increased fluorodeoxyglucose uptake in the uterine mass (Fig. 1, B). Multiple nodules in both lungs were detected on a CT scan (Fig. 1, C).

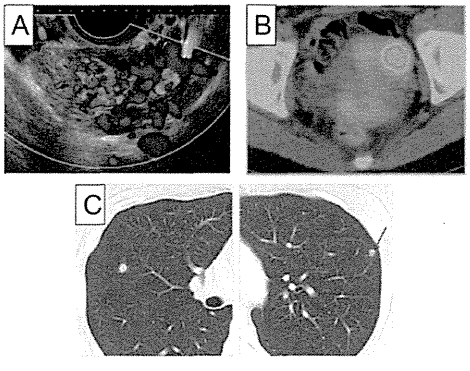

Fig. 1. Imaging findings. (A) Transvaginal Doppler ultrasound results show extensive vascularization within the myometrium. (B) A PET/CT image reveals increased FDG uptake in the mass. (C) A CT image shows multiple nodules in both lungs.

* Corresponding author. Department of Mother-Child Nursing, Faculty of Life Sciences, Kumamoto University, Kuhonji 4-24-1, Chuo-ku, Kumamoto City, Kumamoto 862-0976, Japan.
E-mail address: htashiro@kumamoto-u.ac.jp (H. Tashiro).

http://dx.doi.org/10.1016/j.gore.2015.10.002

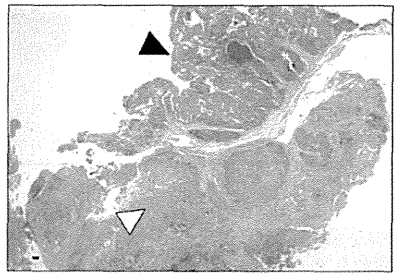

Fig. 2. Histopathological findings of the uterine mass. Choriocarcinoma (►) is composed of basophilic cells and the ETT (▷) contains eosinophilic cells. Tissue was stained with hematoxylin–eosin (HE). Image was taken at 2× magnification. Scale bar = 50 μm.

The tumor presented as a discrete nodule in the myometrium. On microscopic examination, the tumor displayed biphasic proliferation (Fig. 2). Histopathological review of the first excised specimen from the previous hospital confirmed a trophoblastic tumor consisting of the trimorphic proliferation of intermediate trophoblast, syncytiotrophoblast, and cytotrophoblast, with no chorionic villi, and the tumor cells showed abnormal mitotic figures (Fig. 3, A). Tumor cells were diffusely positive for hCG (Fig. 3, B). Although the histological and immunohistochemical findings were characteristics of choriocarcinoma, the tumor was partially composed of cells that were intimately associated with surrounding eosinophilic, hyaline-like material and necrotic debris capable of simulating keratin. The cells contained round, uniform nuclei and eosinophilic or clear cytoplasm surrounded by a well-defined cell membrane (Fig. 4). Immunohistochemical analysis revealed that the tumor cells were diffusely positive for hCG. Those histological features of the component indicated characteristics of ETT notwithstanding the immunopositivity for hCG. Therefore, the patient was diagnosed with choriocarcinoma coexisting with an ETT.

Combination chemotherapy with etoposide, methotrexate and actinomycin-D alternating with cyclophosphamide, and vincristine (EMA-CO) is a standard, effective and well-tolerated regimen for high-risk GTN. MEA also has the same effectiveness as EMA-CO and less toxicity (Matsui et al., 2000), and MEA is one of the standard chemotherapeutic regimens for choriocarcinoma in Japan. She was treated with 6 cycles of combination chemotherapy consisting of MEA. Her serum hCG levels normalized and a follow-up CT scan confirmed that the lung nodules had disappeared. Consequently, she has not undergone additional hysterectomy or chemotherapy, and has had regular menstrual cycles without recurrence in 26 months since the chemotherapy with MEA.

3. Discussion

Our pathological review of the present case showed a mixed choriocarcinoma coexisting with an ETT, which is a rare gestational trophoblastic tumor. In 1998, Shih and Kurman reported 14 cases of mixed choriocarcinoma and ETTs, and in more than half the cases there was a history of either a hydatidiform mole or choriocarcinoma that preceded the diagnosis (Luk and Friedlander, 2013; Shih and Kurman, 1998). Recently, they proposed that choriocarcinoma, PSTT, or ETT may develop as a result of neoplastic transformation of the same cytotrophoblast, which is presumably the trophoblastic stem cell (Shih and Kurman, 2001). This theory explains the existence of gestational trophoblastic neoplasia with mixed histological features, choriocarcinoma, and ETT, as found in the present case.

Although there is extremely limited experience with choriocarcinoma coexisting with an ETT, previous reports suggest that pure-type ETT may not be responsive to the chemotherapeutic agents used in the treatment of other types of GTN (Shih, 2007). A high-dose chemotherapy regimen consisting of cyclophosphamide, etoposide, and carboplatin, however, resulted in a successful outcome in metastatic ETT (Stacey et al., 2002). Once treatment has been completed, most relapses occur within the first year of follow-up, and careful hCG monitoring should be recommended in pure-type ETT (Fieke and Michael, 2014). In this case, serum hCG ultimately rose within 1 month despite an initial response to laparoscopic surgery and MTX under the clinical diagnosis of an ectopic pregnancy, and residual villi without an adequate pathological examination in the previous hospital. Given the potential for the progression of choriocarcinoma coexisting with an ETT after our pathological review, we successfully treated the case with MEA, the chemotherapy regimen for the usual form of choriocarcinoma. Repeated transvaginal ultrasound examinations showed no mass in the uterus, and serum hCG levels have remained negative for over 2 years, conserving fertility.

Here we reported a rare case of choriocarcinoma coexisting with an ETT. The clinical behavior of a mixed choriocarcinoma and ETT seems similar to that of the usual form of choriocarcinoma despite the chemoresistance of pure-type ETT. This case suggests that choriocarcinoma coexisting with an ETT has a high probability of cure with appropriate chemotherapy. Study of additional cases is necessary to reliably determine the behavior of mixed choriocarcinoma coexisting with an ETT, as well as the optimal multimodal treatment approach.

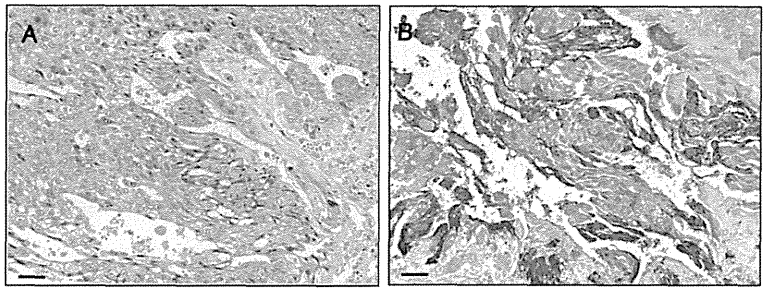

Fig. 3. Histopathological and immunohistological findings of a choriocarcinoma component. Cytological atypia and mitotic figures are numerous. The tumor consists of a trimorphic population of syncytiotrophoblast, intermediate trophoblast and cytotrophoblast (A). The tumor exhibits diffuse immunoreactivity with hCG (B). Tissues were stained with HE (A) and hCG (B). Images were taken at 200× magnification. Scale bar = 50 μm.

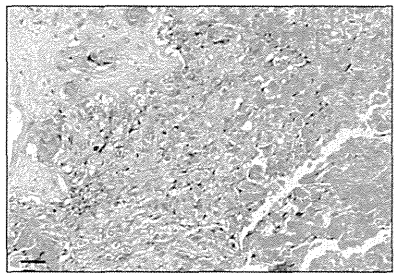

Fig. 4. Histopathological findings of ETT. A nest of tumor cells with a relatively uniform population of mononucleate intermediate trophoblastic cells surrounded by necrotic debris and hyaline degeneration. Tissue was stained with HE. Image was taken at 200× magnification. Scale bar = 50 μm.

Conflict of interest statement

No authors have any conflicts of interest to declare.

References

Fieke, E.M., Michael, J.S., 2014. Gestational trophoblastic tumors: an update for 2014. Curr. Oncol. Rep. 16, 408.
Luk, W.Y., Friedlander, M., 2013. A fibroid or cancer? A rare case of mixed choriocarcinoma and epithelioid trophoblastic tumor. Obstet. Gynecol. 20, 31–47.
Matsui, H., Suzuka, K., Iitsuka, Y., et al., 2000. Combination chemotherapy with methotrexate, etoposide, and actinomycin D for high-risk gestational trophoblastic tumors. Gynecol. Oncol. 78, 28–31.
Shih, I.M., 2007. Gestational trophoblastic neoplasia-pathogenesis and potential therapeutic targets. Lancet Oncol. 8, 642–650.
Shih, I.M., Kurman, R.J., 1998. Epithelioid trophoblastic tumor: a neoplasm distinct from choriocarcinoma and placental site trophoblastic tumor simulationg carcinoma. Am. J. Surg. Pathol. 22, 1393–1403.
Shih, I.M., Kurman, R.J., 2001. The pathology of intermediate trophoblastic tumors and tumor-like lesions. Int. J. Gynecol. Pathol. 20, 31–47.
Stacey, K., Sandra, E.B., Jade, W.Y.C., et al., 2002. Choriocarcinoma and epithelial trophoblastic tumor: successful treatment of relapse with hysterectomy and high-dose chemotherapy with peripheral stem cell support: a case report. Gynecol. Oncol. 85, 204–208.

Cancer Science
Japanese Cancer Association JCA
Open Access

CD44 variant 6 is correlated with peritoneal dissemination and poor prognosis in patients with advanced epithelial ovarian cancer

Francisca Tjhay,[1] Takeshi Motohara,[1] Shingo Tayama,[1] Dashdemberel Narantuya,[1] Koichi Fujimoto,[1] Jianying Guo,[1] Isao Sakaguchi,[1] Ritsuo Honda,[1] Hironori Tashiro[2] and Hidetaka Katabuchi[1]

[1]Department of Obstetrics and Gynecology, Faculty of Life Sciences, Kumamoto University, Kumamoto City, Kumamoto; [2]Department of Maternal-Newborn Nursing, Kumamoto University, Kumamoto City, Kumamoto, Japan

Key words

Cancer stem cell, CD44, ovarian cancer, peritoneal metastasis, prognosis

Correspondence

Takeshi Motohara, Department of Obstetrics and Gynecology, Faculty of Life Sciences, Kumamoto University, Honjo 1-1-1, Chuo-ku, Kumamoto-City, Kumamoto 860-8556, Japan.
Tel: +81-96-373-5269; Fax: +81-96-363-5164;
E-mail: kan@kumamoto-u.ac.jp

Funding Information

This work was supported by grants from the Japan Society for the promotion of Science (grant numbers 15K20151 and 25293344).

Received April 6, 2015; Revised July 13, 2015; Accepted August 3, 2015

Cancer Sci 106 (2015) 1421–1428

doi: 10.1111/cas.12765

Cancer stem cells (CSCs) drive tumor initiation and metastasis in several types of human cancer. However, the contribution of ovarian CSCs to peritoneal metastasis remains unresolved. The cell adhesion molecule CD44 has been identified as a major marker for CSCs in solid tumors, including epithelial ovarian cancer. CD44 exists as a standard form (CD44s) and also as numerous variant isoforms (CD44v) generated by alternative mRNA splicing. Here we show that disseminated ovarian tumors in the pelvic peritoneum contain highly enriched CD44v6-positive cancer cells, which drive tumor metastasis and are responsible for tumor resistance to chemotherapy. Clinically, an increased number of CD44v6-positive cancer cells in primary tumors was associated with a shortened overall survival in stage III–IV ovarian cancer patients. Furthermore, a subpopulation of CD44v6-positive cancer cells manifested the ability to initiate tumor metastasis in the pelvic peritoneum in an *in vivo* mouse model, suggesting that CD44v6-positive cells show the potential to serve as metastasis-initiating cells. Thus, the peritoneal disseminated metastasis of epithelial ovarian cancer is initiated by the CD44v6-positive subpopulation, and CD44v6 expression is a biomarker for the clinical outcome of advanced ovarian cancer patients. Given that a distinct subpopulation of CD44v6-positive cancer cells plays a critical role in peritoneal metastasis, definitive treatment should target this subpopulation of CD44v6-positive cells in epithelial ovarian cancer.

Epithelial ovarian cancer is the leading cause of death from gynecological malignancies.[1] Because most patients with ovarian malignancies are generally asymptomatic until the cancer has progressed and metastasized, more than two-thirds of tumors are diagnosed at an advanced stage with multiple disseminated tumors in the pelvic peritoneum.[2] The clinical outcomes for women diagnosed with advanced epithelial ovarian cancer are poor even after treatment with extirpative surgery and proper chemotherapy. Although the cancer may respond to primary therapy, chemoresistant residual cancer cells can persist in a dormant state for many months in the pelvic peritoneum, leading to relapse.[3,4] Therefore, elucidating the molecular events that control peritoneal metastasis may provide potential molecular targets for the treatment of advanced epithelial ovarian cancer with multiple peritoneal disseminated tumors.

Cell adhesion molecule CD44 is a polymorphic integral membrane glycoprotein that binds hyaluronic acid and contributes to tumor growth, invasion, and metastasis.[5–7] CD44 exists as a standard form (CD44s) and also as numerous variant isoforms (CD44v) generated by alternative mRNA splicing of up to 10 variant exons that encode parts of the extracellular domain.[6–10] Among CD44v isoforms, CD44v6 was initially found to promote the metastatic potential of a rat pancreatic adenocarcinoma cell line.[11] Furthermore, several previous studies supported the premise that CD44v6 plays a key role in cancer proliferation, migration, and invasion in a variety of human cancers, such as colorectal, breast, lung, and ovarian cancer.[12–15] In epithelial ovarian cancer, it is known that CD44v6 promotes tumor metastasis by binding hyaluronic acid on peritoneal mesothelial cells.[16]

In recent history, the cancer stem cell (CSC) theory has proposed that the bulk of tumor cells are generated by a rare population of tumor-initiating cells, conceptually termed CSCs.[17–19] CSCs possess the ability to self-renew and differentiate into a heterogeneous lineage of cancer cells and inherently drive the metastatic process.[18,20] CD44 has been identified as one of the major cell surface markers associated with CSCs in several types of epithelial tumors, including ovarian cancer.[6,21–23] Intriguingly, recent studies indicated that a subpopulation of CD44v6-positive cells shows a characteristic phenotype of CSCs in colorectal cancer, bladder cancer, and brain tumor.[24–26] These findings led us to hypothesize that CD44v6-positive ovarian cancer cells may possess CSC traits and play a key role in tumor initiation and disseminated metastasis.

Uncovering the molecular mechanisms underlying peritoneal metastasis is the final frontier in ovarian cancer biology. Even

though ovarian CSCs have not been fully elucidated, these cells are thought to play a crucial role in disseminated metastasis and relapse at peritoneal metastatic sites.[27] The present study was designated to evaluate the role of CD44v6 in peritoneal disseminated metastasis and the potential relevance of CD44v6 to the clinical outcome of patients with advanced epithelial ovarian cancer with long-term follow-up.

Materials and Methods

Patients and tissue preparation. From January 2002 to December 2012, the clinical records of stage III–IV epithelial ovarian cancer patients were reviewed retrospectively, and 59 patients with peritoneal disseminated tumors who underwent primary standard surgery followed by proper chemotherapy at Kumamoto University Hospital were included in this study. Patients were excluded when they had borderline tumors, multiple primary cancers, or non-epithelial tumors. The eligible patients were followed-up until December 2014. Written informed consent was obtained from all patients before treatment, in accordance with the institutional guidelines of our hospital.

Tumor tissues obtained surgically were fixed in 10% buffered formalin, embedded in paraffin, and sectioned at 4-μm thickness for histological diagnosis. Sections were stained with H&E, and histologic typing was carried out according to the WHO classification of surface epithelial–stromal ovarian tumors.[28] All tumors were staged according to the International Federation of Gynecology and Obstetrics criteria.[29]

Evaluation of immunohistochemical staining. Immunohistochemical analysis was carried out as described previously.[30] Briefly, the sections were washed with PBS, subjected to antigen retrieval by heating in a microwave in 0.01 M sodium citrate buffer (pH 6.0) for 15 min, and exposed to 3% H_2O_2 in methanol before staining with the primary antibody. Immune complexes were detected with use of the avidin–biotin–peroxidase complex (ABC kit; Vector Laboratories, Burlingame, CA, USA) and diaminobenzidine substrate (Vector Laboratories), and the sections were counterstained with hematoxylin. CD44v6 was detected with the mouse mAb CD44v6 (2F10; R&D Systems, Minneapolis, MN, USA). The expression level of CD44v6 was quantified as a percentage of the total number of stained cells. The primary ovarian tumors that contained at least 10% CD44v6-positive cancer cells were categorized as the "CD44v6-high" group, whereas the tumors that contained less than 10% CD44v6-positive cells were categorized as the "CD44v6-low" group. The percentage of CD44v6-positive cancer cells in primary tumors was evaluated by counting cells in at least three microscopic fields per slide.

Mice. BALB/c nude mice were obtained from CLEA (Tokyo, Japan) and maintained according to institutional guidelines. All animal experiments were carried out in accordance with protocols approved by the animal ethics committee of Kumamoto University.

Cell line. A human ovarian cancer cell line, ES-2, was obtained from ATCC (Manassas, VA, USA). ES-2 cells were maintained in RPMI-1640 medium (Wako Pure Chemical Industries, Osaka, Japan) supplemented with 10% FBS at 37°C in a 5% CO_2-containing atmosphere.

Flow cytometry and transplantation assay. Cell sorting and flow cytometric analysis were carried out with the use of a FACS Aria II (BD Biosciences, San Jose, CA, USA). Cells were incubated with allophycocyanin-conjugated mouse mAb CD44v6 (2F10; R&D Systems) and phycoerythrin-conjugated rat mAb CD44 (IM7; BioLegend, San Diego, CA, USA) for 30 min. The FACS-sorted CD44v6-positive or -negative cancer cells were suspended in RPMI-1640 medium and injected i.p. into 7-week-old female BALB/c nude mice. Tumor-initiating frequencies were assessed with the use of ELDA software for limiting dilution analysis.[31]

Immunoblot analysis. Immunoblot analysis was carried out as previously described.[27] In brief, equal amounts of cell lysate protein were subjected to SDS-PAGE, transferred to a nitrocellulose membrane, and exposed to anti-CD44v6 antibody (VFF-18; Abcam, Cambridge, UK), anti-E-cadherin (36/E-cadherin; BD Biosciences), anti-N-cadherin (32/N-cadherin; BD Biosciences), anti-fibronectin (10/fibronectin; BD Biosciences), anti-vimentin (V9; DakoCytomation, Glostrup, Denmark), and anti-β-actin (13E5; Cell Signaling Technology, Beverly, MA, USA). Immune complexes were visualized by chemiluminescence detection (Pierce Biotechnology, Rockford, IL, USA).

Proliferation and chemosensitivity assay. Cell viability was assessed with MTS assay according to the manufacturer's protocol (CellTiter 96 Aqueous One Solution Cell Proliferation assay; Promega, Madison, WI, USA). Briefly, cells (3×10^3/100 μL per well) were plated in 96-well flat bottom plates and serum starved overnight. Ovarian cancer cells were treated with paclitaxel or cisplatin at the indicated concentrations. At 12 h post-drug treatment, 20 μL MTS assay solution was added to each well for 2 h. Absorbance was recorded at 490 nm on an SpectraMax 190 microplate reader (Molecular Devices, Sunnyvale, CA, USA). Experiments were carried out in triplicate and repeated three times and the percentage of cell survival was defined as the relative absorbance of untreated versus treated cells.

Statistical analysis. The prognosis of patients was determined according to the cumulative survival rate after treatment. Survival rates were calculated using the Kaplan–Meier method, and differences between curves were assessed with the log-rank test. Correlations between variables were evaluated with the χ^2-test, Fisher's exact test, Mann–Whitney *U*-test, or Wilcoxon test. Data are presented as mean ± SD and were analyzed with the Student's *t*-test. Univariate and multivariate Cox proportional hazard model analyses were carried out to calculate hazard ratios (HRs) using SPSS version 21.0 (IBM, Armonk, NY, USA). In all analyses, a *P*-value of <0.05 was considered statistically significant.

Results

Correlation between CD44v6 expression pattern and clinicopathological features in patients with stage III–IV epithelial ovarian cancer. The association between CD44v6 expression and the clinicopathological characteristics of the 59 patients is shown in Table 1. Thirteen (22.0%) cases belonged in the CD44v6-high group, and 46 (78.0%) cases to the CD44v6-low group. The median age of all patients at diagnosis was 57 years (range, 37–82 years). There were no significant differences in the median age between the CD44v6-high and CD44v6-low groups. In addition, no significant correlation was observed between the immunohistochemical (IHC) expression of CD44v6 and clinicopathological characteristics, such as tumor histological type, tumor marker CA125, and tumor size. Adjuvant systematic chemotherapy was given as clinically indicated in accordance with standard practices, and almost all patients (57/59, 96.6%) received paclitaxel–carboplatin as first-line adjuvant chemotherapy. No significant differences were recorded in the distribution of the number of cycles of

Table 1. Association between CD44 variant 6 (CD44v6) expression pattern and clinicopathological characteristics in patients with stage III–IV ovarian cancer

	All cases, *n* (%)	CD44v6-high group, *n* (%)	CD44v6-low group, *n* (%)	*P*-value
All cases	59	13	46	
Median age, years (range)	57 (37–82)	59 (43–82)	56 (37–77)	0.84
Age, years				
<50	18 (30.5)	3 (23.1)	15 (32.6)	0.51
≥50	41 (69.5)	10 (76.9)	31 (67.4)	
Histological type				
Serous	42 (71.2)	7 (53.8)	35 (76.1)	0.12
Clear	3 (5.1)	2 (15.4)	1 (2.2)	
Endometrioid	5 (8.5)	1 (7.7)	4 (8.7)	
Mucinous	1 (1.7)	1 (7.7)	0 (0.0)	
Mixed	7 (11.8)	1 (7.7)	6 (13.0)	
Undifferentiated	1 (1.7)	1 (7.7)	0 (0.0)	
CA125, U/mL				
<500	18 (30.5)	6 (46.2)	12 (26.1)	0.16
≥500	41 (69.5)	7 (53.8)	34 (73.9)	
Tumor size, cm				
<10	40 (67.8)	7 (53.8)	33 (71.7)	0.22
≥10	19 (32.2)	6 (46.2)	13 (28.3)	
First-line chemotherapy regmen				
Paclitaxel/ carboplatin	57 (96.6)	12 (92.3)	45 (97.8)	0.33
Other	2 (3.4)	1 (7.7)	1 (2.2)	
No. of cycles of chemotherapy				
<2	41 (69.5)	8 (61.5)	33 (71.7)	0.48
≥3	18 (30.5)	5 (38.5)	13 (28.3)	

chemotherapy between CD44v6-high and CD44v6-low groups (Table 1).

Highly enriched CD44v6-positive ovarian cancer cells in peritoneal disseminated tumors. To investigate whether CD44v6-positive cancer cells are associated with peritoneal metastasis, we compared the average number of CD44v6-positive cells among the 59 samples of primary ovarian tumors to that in samples of peritoneal disseminated tumors taken from the same patients. Representative IHC staining patterns for CD44v6 in primary and disseminated tumors are shown in Figure 1(a,b). Immunohistochemical analysis revealed a significantly higher percentage of CD44v6-positive cells detected in peritoneal disseminated tumors than in corresponding primary ovarian tumors ($P < 0.01$; Fig. 1c). These findings indicated that CD44v6-positive cells are correlated with peritoneal dissemination, and the pelvic peritoneum may have the potential to form a part of the niche microenvironment involved in tumor initiation and metastasis.

Prognostic impact of CD44v6 expression in advanced epithelial ovarian cancer patients. Given that a subpopulation of CD44-positive cancer cells in hierarchically organized ovarian cancer manifests CSC properties,[21] we hypothesized that CD44v6 expression would correlate with aspects of ovarian cancer survival. To address this issue, we used Kaplan–Meier analyses of overall survival (OS) and progression-free survival (PFS) between the CD44v6-high and CD44-low groups. Representative IHC staining patterns for CD44v6 in CD44-high and CD44-low groups are shown in Figure 2(a, b). In the evaluation of the sites of primary lesions, the 5-year OS rates were 18.0% (95% confidence interval [CI], 0.0–40.2) in the CD44-high group and 59.6% (95% CI, 44.3–74.8) in the CD44-low group. Significant differences

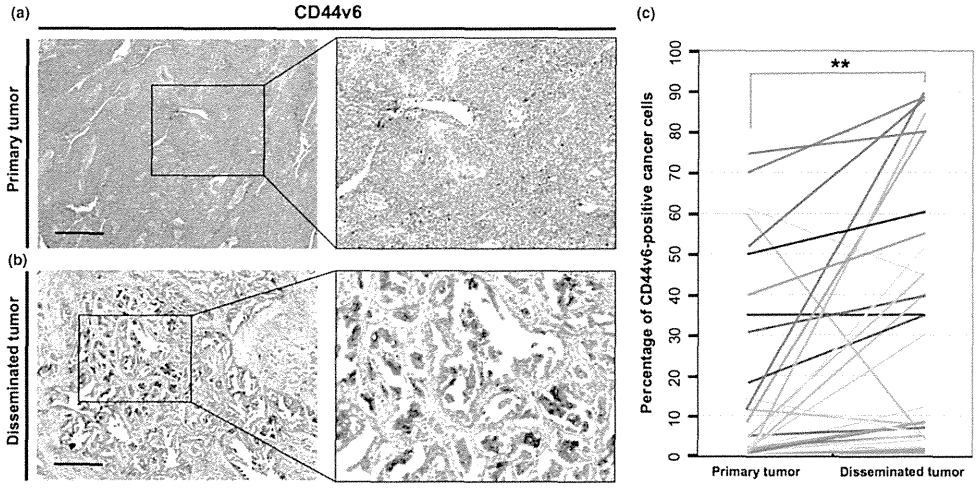

Fig. 1. Disseminated ovarian tumors in the pelvic peritoneum contain highly enriched CD44 variant 6 (CD44v6)-positive cancer cells. (a) Immunohistochemical analysis with an anti-CD44v6 antibody in primary epithelial ovarian tumors. Scale bar = 500 μm. (b) Immunohistochemical staining with an anti-CD44v6 antibody in peritoneal disseminated tumors. Scale bar = 500 μm. (c) The percentage of CD44v6-positive cancer cells in primary and disseminated tumors. Peritoneal disseminated tumors contained significantly higher percentages of CD44v6-positive cells than primary tumors (Mann–Whitney *U*-test, $^{**}P < 0.01$).

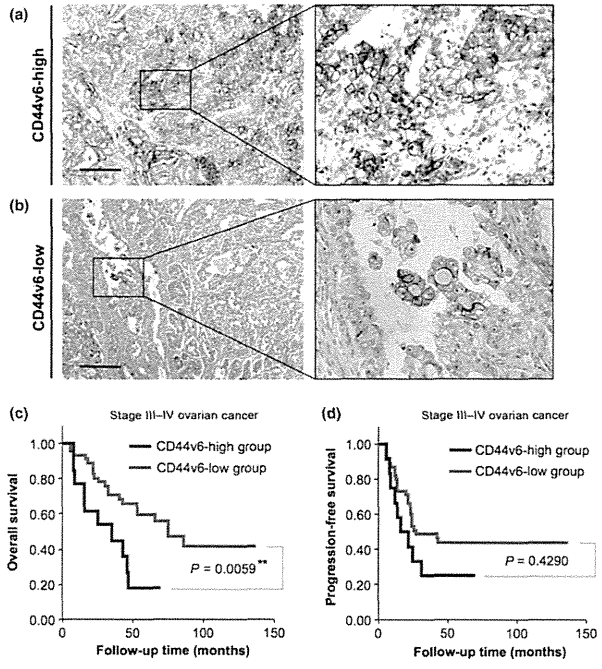

Fig. 2. CD44 variant 6 (CD44v6) expression predicts epithelial ovarian cancer survival. (a) Immunohistochemical analysis with an anti-CD44v6 antibody in primary epithelial ovarian tumors. The tumors that contained at least 10% CD44v6-positive cancer cells were categorized as the CD44v6-high group. Scale bar = 500 μm. (b) Immunohistochemical staining with an anti-CD44v6 antibody in primary tumors. The tumors that contained less than 10% CD44v6-positive cancer cells were categorized as the CD44v6-low group. Scale bar = 500 μm. (c) Kaplan–Meier analysis of overall survival in patients with stage III–IV ovarian cancer according to the expression of CD44v6. There were significant differences in overall survival between the CD44v6-high and CD44v6-low groups (**P = 0.0059). (d) Kaplan–Meier analysis of progression-free survival in patients with stage III–IV ovarian cancer according to the expression of CD44v6. Progression-free survival was not significantly different between the CD44v6-high and CD44v6-low groups (P = 0.4290).

Table 2. Hazard ratios (HRs) using univariate and multivariate Cox proportional hazard model

Prognostic factor	Univariate analysis			Multivariate analysis		
	HR	95% CI	*P*-value	HR	95% CI	*P*-value
Age, years						
<50						
≥50	1.286	0.574–2.879	0.542			
CA125, U/mL						
<500						
≥500	1.060	0.487–2.306	0.884			
Tumor size, cm						
<10						
≥10	1.063	0.498–2.267	0.874			
First-line chemotherapy						
Paclitaxel/carboplatin						
Other	0.905	0.122–6.727	0.923			
Surgical debulking status						
Optimal surgery (Residual tumor size <1 cm)						
Suboptimal surgery (Residual tumor size ≥1 cm)	2.568	1.247–5.288	0.011	2.283	1.091–4.775	0.028
CD44v6 expression						
Low						
High	2.930	1.334–6.436	0.007	2.568	1.149–5.738	0.022

CD44v6, CD44 variant 6; CI, confidence interval; High,; Low,.

were observed in OS between the CD44v6-high and CD44v6-low groups for patients with stage III–IV ovarian cancer (P = 0.0059; Fig. 2c). In contrast, no significant differences were observed in PFS between the CD44v6-high and CD44v6-low groups (P = 0.4290; Fig. 2d). These findings suggested that CD44v6-positive cancer cells in primary

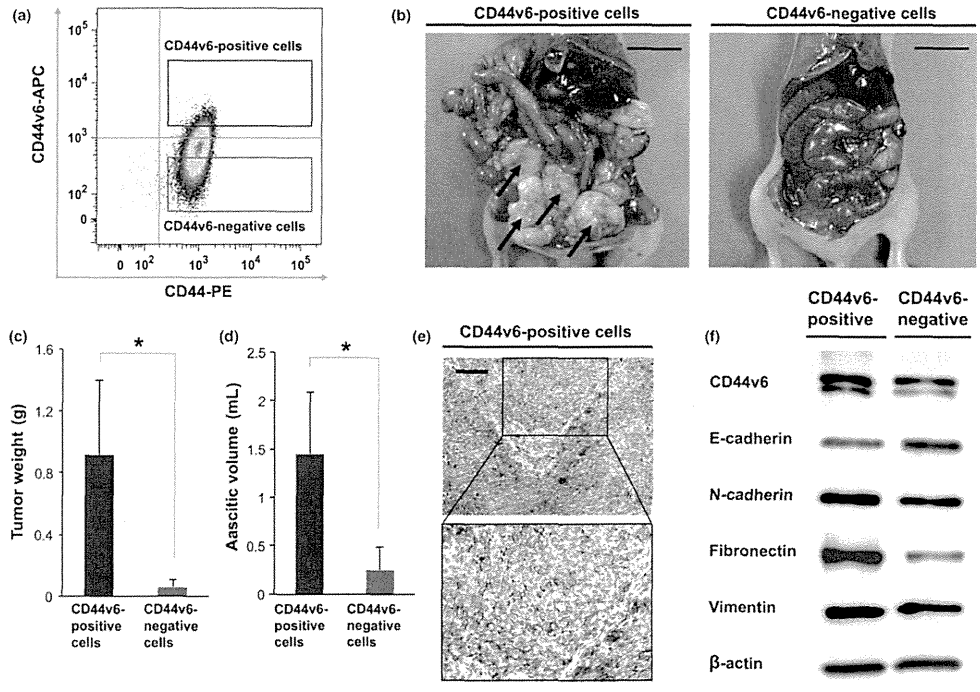

Fig. 3. Subpopulation of CD44 variant 6 (CD44v6)-positive ovarian cancer cells possesses a high peritoneal metastatic ability. (a) Flow cytometric analysis of CD44v6 expression in ES-2 ovarian cancer cells. (b) Macroscopic appearance of disseminated tumors at 35 days after cell transplantation. CD44v6-positive cells generated more extensive disseminated tumors in the peritoneal cavity than CD44v6-negative cells. Scale bar = 2 cm. (c) Total weight of peritoneal disseminated tumors determined at 35 days after cell injection. Quantitative data are presented as mean ± SD for five mice. *$P < 0.05$. (d) Ascitic volume determined at 35 days after transplantation. Quantitative data are presented as mean ± SD for five mice. *$P < 0.05$. (e) Immunohistochemical analysis with antibody to CD44v6 in peritoneal disseminated tumors in a mouse model. Paraffin-embedded sections of disseminated tumors generated by CD44v6-positive cancer cells were subjected to immunohistochemical staining with an anti-CD44v6 antibody. Scale bar = 200 μm. (f) Western blot analysis of CD44v6 and epithelial–mesenchymal transition regulatory proteins, including E-cadherin, N-cadherin, fibronectin, and vimentin in FACS-sorted CD44v6-poisitive cells *versus* FACS-sorted CD44v6-negative cells.

tumors play an important role in the survival of advanced ovarian cancer patients.

Univariate and multivariate analysis of various clinicopathological factors in relation to OS are shown in Table 2. Immunohistochemical expression of CD44v6 proved to be a highly predictive factor based on the univariate Cox proportional hazards model ($P = 0.007$; HR, 2.930; 95% CI, 1.334–6.436) and the multivariate Cox proportional hazards model ($P = 0.022$; HR, 2.568; 95% CI, 1.149–5.738). In addition, surgical debulking status also significantly correlated with OS based on the univariate Cox proportional hazards model ($P = 0.011$; HR, 2.568; 95% CI, 1.247–5.288) and the multivariate Cox proportional hazards model ($P = 0.028$; HR, 2.283; 95% CI, 1.091–4.775).

High metastatic ability in a subpopulation of CD44v6-positive ovarian cancer cells. Given that CD44v6-positive cancer cells showed high metastatic potential in patients with advanced ovarian cancer, we next examined the relevance of peritoneal metastasis in a subpopulation of CD44v6-positive cells in an *in vivo* mouse model. To compare the peritoneal metastatic abilities of CD44v6-positive and CD44v6-negative cancer cells, we sorted CD44v6-positive and CD44v6-negative cells from the ES-2 ovarian cancer cell line (Fig. 3a) and serially transplanted them intraperitoneally into nude mice. Limiting dilution assay revealed that CD44v6-positive cells had a greater tumor initiating ability than CD44v6-negative cells, suggesting that a subpopulation of CD44v6-positive cells is highly efficient at metastatic dissemination (Table 3). The CD44v6-positive cells generated extensive disseminated tumors, resulting in massive abdominal distension by hemorrhagic ascites, within 5 weeks of inoculation, whereas CD44v6-negative cells showed little ability to form disseminated tumors in the peritoneal cavity (Fig. 3b). The total weight of peritoneal disseminated tumors formed by CD44v6-positive cells was significantly greater than that of those formed by CD44v6-negative cells ($P < 0.05$; Fig. 3c). In addition, transplantation of CD44v6-positive cells caused a significant increase in the ascitic volume in comparison with that resulting from transplantation of CD44v6-negative cells ($P < 0.05$; Fig. 3d). A representative IHC staining pattern for CD44v6 in peritoneal disseminated tumors generated by CD44v6-positive cancer cells is shown in Fig-